Original Article
Effects of Astragalus polysaccharide on the structure and function of skeletal muscle in D-galactose-induced C57BL/6J mice

Deqing Chen, Yongxin Wu, Yingxiao Zhang, Hailing Yang, Qian Xiao

Department of Geriatrics, The First Affiliated Hospital of Chongqing Medical University, Chongqing 400042, China

Abstract: Objective: To investigate the effects of Astragalus polysaccharide (APS) on skeletal muscle structure and function in D-galactose (D-gal)-induced C57BL/6J mice. Methods: Eighteen male C57BL/6J mice of specific pathogen-free (SPF) grade, aged 8 weeks, were selected and divided into three groups: a control group (0.9% saline gavage for 16 weeks), a D-gal group (subcutaneous injection of 200 mg/kg D-galactose in the upper neck region, once daily for 8 weeks), and a D-gal + APS group (subcutaneous injection of 200 mg/kg D-galactose, once daily for 8 weeks, with concurrent administration of 100 mg/kg APS by gavage for 8 weeks). Body composition of the mice was assessed using the ImpediVET Laboratory Composition Measurement Analyzer. The pathological structure of the skeletal muscles was examined using hematoxylin and eosin (HE) staining, and the microstructure and mitochondrial alterations in skeletal muscle were observed under transmission electron microscopy. Protein expression levels of LC3II and PINK1 in skeletal muscle tissues were analyzed using Western blotting analysis. Results: Compared to the control group, the D-gal-treated mice demonstrated substantial declines in grip strength, the cross-sectional area (CSA) of gastrocnemius muscle fibers, gastrocnemius weight, and the gastrocnemius weight-to-body weight ratio. APS administration markedly improved these parameters in the D-gal-treated mice. H&E staining showed muscle atrophy and senescence in the D-gal-treated mice, accompanied by deformed muscle cell morphology, which was mitigated by APS gavage. The D-gal-treated mice displayed swelling, cristae fracture, lysis, or complete loss, alongside reduced autophagy and increased lengths of bright bands, myofibrillar myonules, and H bands. However, administration of APS alleviated mitochondrial damage, promoted mitophagy, and reduced the lengths of these muscle tissue bands. Additionally, D-gal treatment significantly reduced LC3II and PINK1 protein expression in muscle tissues, while APS treatment notably elevated their expression levels. Conclusion: APS gavage ameliorates the structural and functional impairments in muscle tissues of the D-gal-treated mice by promoting mitochondrial autophagy.

Keywords: D-galactose, Astragalus polysaccharide, skeletal muscle, C57BL/6J mice

Introduction

Sarcopenia, as defined by the European Sarcopenia Working Group, is a progressive decline in skeletal muscle mass and strength, resulting in various disabilities, reduced quality of life, and even mortality. This generalized disorder of skeletal muscles significantly increases the risk of falls, fractures, disability, and mortality in those affected [1, 2]. With the gradual aging of the global population, the incidence of sarcopenia has been steadily rising [3]. Existing data reveal that the prevalence of sarcopenia among individuals aged 60-70 years is approximately 5%-13%, with prevalence rising to 11%-50% in those aged 80 and above. Among the Asian population, the prevalence ranges from 4.1% to 11.5% [3]. The World Health Organization (WHO) predicts that within the next 40 years, over 200 million people will be afflicted by sarcopenia, making it a significant public health concern worldwide [2].

The underlying mechanisms of sarcopenia remain unclear. Several studies [4, 5] indicate a complex interplay of factors such as inflammation, diminished physical activity, inadequate protein consumption, and the natural aging.

Nevertheless, differentiating the individual impacts of aging, chronic diseases, physical inactivity, and insufficient protein intake on the progression of sarcopenia poses a significant challenge. Autophagy, a crucial cellular housekeeping mechanism responsible for degrading cytoplasmic components such as protein aggregates and organelles, has been implicated in the pathogenesis of sarcopenia. Dysfunction in autophagy-dependent signaling has been observed in patients with sarcopenia. Liang et al. [6] demonstrated that appropriate exercise can induce autophagy or regulate its functional state, implying that exercise-induced autophagy may play a pivotal in mitigating sarcopenia. Exercise-induced autophagy has emerged as an effective therapeutic measure to slow the progression of sarcopenia, improve mitochondrial mass, and boost the number of quiescent satellite cells [6]. Moreover, Zeng et al. [7] found that exercise induces autophagy and enhances mitochondrial quality by regulating the Akt/mTOR and Akt/FoxO3a signaling pathways in a sarcopenia rat model. These findings suggest that exercise-induced autophagy serves as a potent therapeutic approach for alleviating sarcopenia. Collectively, these studies provide a theoretical foundation for the present research.

Astragalus is known for its properties to strengthen the spleen, aid digestion, enhance immunity, as well as consolidate and fortify the exterior. Astragalus polysaccharide (APS), a water-soluble heteropolysaccharide extracted and purified from the dried root of Astragalus, comprises fructose, glucose, rhamnose, arabinose, and hexuronic acid. Pharmacological experiments have confirmed that [8] APS possesses antiviral, antitumor, anti-ageing, and antioxidant properties.

Currently, the pharmacological treatment of sarcopenia remains in its nascent stages, with few specific therapeutic options available globally. In this study, mice were treated with D-gal to simulate the progression of sarcopenia in vivo, and APS was administered via gavage to evaluate the effects of APS on skeletal muscle structure, function, and autophagy in the D-gal-treated mice, thereby providing a clinical reference for the pharmacological treatment of sarcopenia.

Experimental methods

Construction of a mouse model of sarcopenia

Eight-week-old male C57BL/6J mice were raised under a controlled environment, maintained at a constant temperature of 22±2°C, with a relative humidity of 60%, a 12-hour light/dark cycle, and ambient noise levels kept below 60 dB. The mice were provided with ad libitum access to water and food.

The mice were weighed and randomly allocated into three groups: a saline control group (Control), a D-galactose-induced sarcopenia model group (D-gal), and a D-galactose model supplemented with APS treatment group (D-gal + APS), comprising six mice in each group. For D-gal treatment, 12 mice received a subcutaneous injection of 200 mg/kg D-galactose in the upper neck once daily for 8 weeks. The control group received an equivalent dose of saline injection. The modeling of sarcopenia was considered successful when the Sarcopenia Index (SI), defined as the ratio of target skeletal muscle mass (mg) to body weight (g), fell below twice the standard deviation of normal mice [9]. The study was approved by the Animal Care and Use Committee of the First Affiliated Hospital of Chongqing Medical University.

Following the validation of the sarcopenia model, six mice from the D-gal-treated group were chosen for APS intervention. These mice underwent APS treatment via gavage at 100 mg/kg for 8 weeks, while continuing D-galactose injections at 200 mg/kg in the upper neck. Concurrently, mice in the control and D-gal groups were administered equivalent volumes of saline via gavage or continued their D-galactose injections (**Table 1**).

Outcome measurements

Grip strength test: The grip strength of the mice was measured using a YLS-13A grip strength meter. First, the device was activated. The mouse was carefully held by the back and gently placed on the grip strength apparatus. The mouse's tail was gently secured and pulled backward, allowing the mouse to grip the grid firmly with its paws. The pulling force was gradually increased until the mouse released its grip, and the maximal pulling force displayed on

Table 1. Grouping and intervention

Group	Number of animals	Mode of administration	Duration of administration (weeks)
Control	6	Subcutaneous injection of 0.2 ml saline in the upper neck	16
D-gal	6	Subcutaneous injection of 200 mg/kg D-gal in the upper neck	16
D-gal + APS	6	Subcutaneous injection of 200 mg/kg D-gal in upper neck + 100 mg/kg of APS by gavage	8+8

D-gal, D-galactose; APS, Astragalus polysaccharide.

the device was recorded. Each mouse was subjected to 10 trials, and the mean value of these trials was calculated for analysis [10].

Body mass analysis and gastrocnemius muscle sampling: The body weight of each group of mice was measured, followed by the administration of sodium pentobarbital through intraperitoneal injection at a dose of 80 mg/kg to induce anesthesia, after which euthanasia was performed using cervical dislocation. The mice were positioned on a foam board, and a thoracotomy was conducted to expose the heart. An incision was made in the right atrium, and saline was perfused through the heart until the liver and kidneys appeared blanched. Subsequently, an incision was made in the right hind limb to expose the underlying skeletal muscles.

The gastrocnemius muscle, located posterior to the tibia and fibula, was identified and isolated. Using forceps, the muscles surrounding the gastrocnemius were delicately separated and excised, exposing the entire gastrocnemius muscle. The muscle was subsequently detached from the tendon with scissors, and the proximal attachment was carefully separated. The soleus muscle, located posterior to the gastrocnemius, was also dissected, and the gastrocnemius muscle was fully detached near its proximal attachment. Any non-experimental muscle tissue adhering to the tibia and fibula was excised, and the tibial bones were exposed and collected following their fracture at the joints.

This procedure was repeated on the left hind limb to obtain the gastrocnemius muscle and tibia. The harvested gastrocnemius muscles were weighed using an analytical balance. The right gastrocnemius muscle was stored at -80°C for subsequent experiments, while the left gastrocnemius muscle was fixed in 4% paraformaldehyde for histological analysis. Subsequently, the weight of the gastrocnemius muscle and the ratio of its weight to body weight were calculated.

Paraffin embedding of gastrocnemius muscle tissue: Tissue blocks (0.5 cm × 0.5 cm × 0.5 cm) were excised from the midsection of the gastrocnemius muscle and fixed in a 10% neutral formaldehyde solution for 16 h. Subsequently, the tissues were subjected to gradient alcohol dehydration utilizing various concentrations of ethanol: 70% ethanol for 24 h, 80% ethanol for 12 h, 90% ethanol for 2 h, 95% ethanol I and II for 2 h each, 100% ethanol for 1 h, 100% ethanol for 0.5 h, xylene I for 5 min, xylene II for 3 min. Following dehydration, the tissue was embedded in paraffin wax I for 2 h and paraffin wax II for 2 h, ensuring the cross-section faced downward. The embedded tissues were then cooled at room temperature and stored in a refrigerator at 4°C until further use.

Hematoxylin-eosin staining: The gastrocnemius muscle tissues, fixed in 10% neutral formaldehyde, were dehydrated and embedded in paraffin. Thin sections of the embedded tissues were prepared using a microtome. These sections were deparaffinized and subsequently stained with hematoxylin reagent for 10 min. Following staining, the sections were rinsed under running tap water for 3 min to remove excess staining reagent. They were then differentiated in hydrochloric acid alcohol for 10 s, rinsed again under running tap water for 3 min, and immersed in warm water at 50°C until the sections turned blue. After another 3-minute rinse under running tap water, the sections were transferred to 85% alcohol for 3 min. The tissues were then stained with eosin reagent for 5 min, followed by a 3-minute rinse under running tap water. Next, the sections were dehydrated through a series of graded alcohols, cleared with xylene, sealed, and observed under a microscope. The cross-sectional area (CSA) of gastrocnemius muscle fibers was analyzed and quantified utilizing ImageJ software.
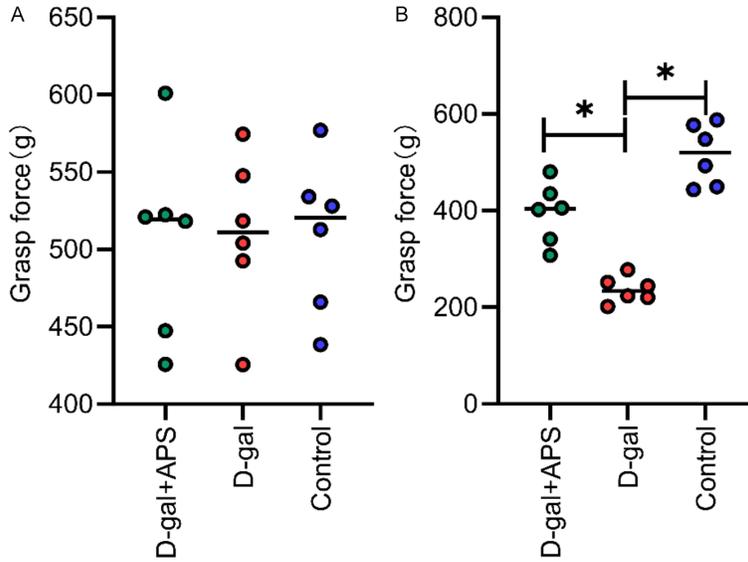
Figure 1. Effect of APS on the grip strength of D-gal-treated mice. A. There was no significant difference in grip strength among the three groups of mice before intervention (n=6 for each group) (*P*>0.05). B. After intervention, D-gal treatment significantly reduced the grip strength of the mice compared to the control group (*P*<0.05), whereas APS treatment significantly increased the grip strength compared to the D-gal group (*P*<0.05). D-gal, D-galactose; APS, Astragalus polysaccharide.
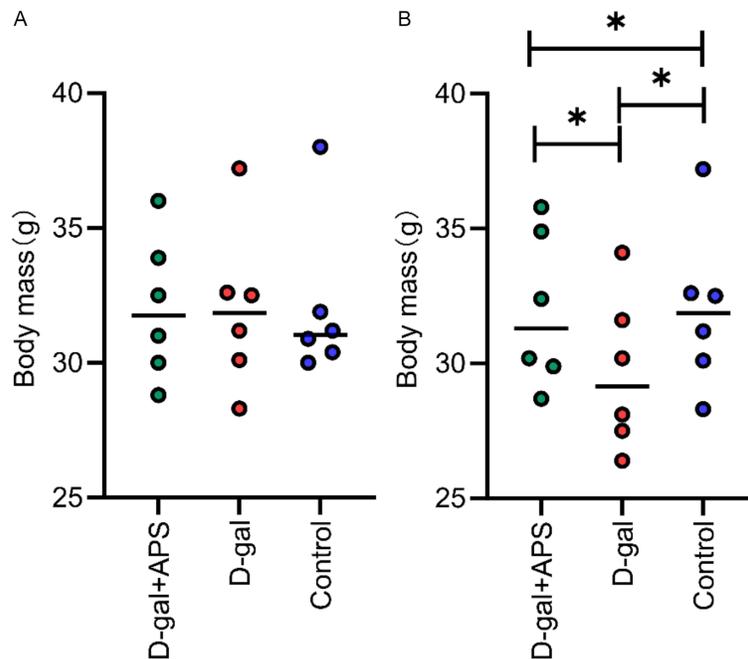
Figure 2. Effect of APS on body mass of D-gal-treated mice. A. There was no statistically significant difference in body mass among the three groups before intervention (n=6 for each group) (*P*>0.05). B. After intervention, the body mass decreased in the D-gal group compared to the control group, and ASP treatment significantly increased the body mass compared to the D-gal group (*P*<0.05). APS, Astragalus polysaccharide; D-gal, D-galactose.

Transmission electron microscopy (TEM) experiments: Muscle tissue samples were initially fixed with glutaraldehyde for 24 h, followed by post-fixation with 1% osmium tetroxide for an additional 24 h. Subsequently, the fixed samples underwent dehydration utilizing a graded series of acetone solutions. The dehydrated samples were then permeabilized with a mixture of acetone and epoxy resin. The processed tissue blocks were transferred into pre-prepared molds containing embedding solution and polymerized with heat to form solid embedded blocks. Ultra-thin sections were prepared using an ultramicrotome. The sections were stained with uranyl acetate for 15 min, followed by staining with lead citrate for 2 min at room temperature. The JEM-1400PLUS transmission electron microscope was employed to observe the ultrastructural changes in mitochondrial constructs and organelles, as well as changes in the length of the sarcomere, the A-band, the I-band, and the H-band in the muscle tissue of the mice.

Western blot analysis: To prepare the lysate, 10 μL of phosphatase inhibitor, protease inhibitor, and PMSF were added to 1 mL of cold lysis buffer. The mixture was thoroughly homogenized and kept on ice for subsequent use. Muscle tissues were extracted from the mice and lysed using the freshly prepared lysis buffer. The cell lysates were transferred to a 1.5 mL EP tube and centrifuged at 12,000 g for 30 min at 4°C. The supernatant was collected for total
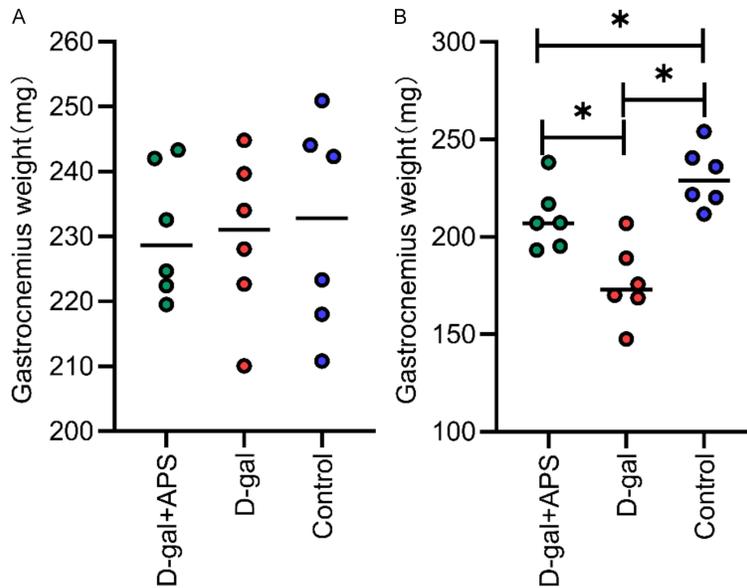
Figure 3. Effect of APS on gastrocnemius muscle weight in D-gal-treated mice. A. There was no statistically significant difference in gastrocnemius muscle weight among the three groups before intervention (n=6 for each group) (*P*>0.05). B. After intervention, the gastrocnemius muscle weight decreased in the D-gal group compared to the control group, and ASP treatment significantly increased gastrocnemius muscle weight compared to the D-gal group (*P*<0.05). D-gal, D-galactose; APS, Astragalus polysaccharide.
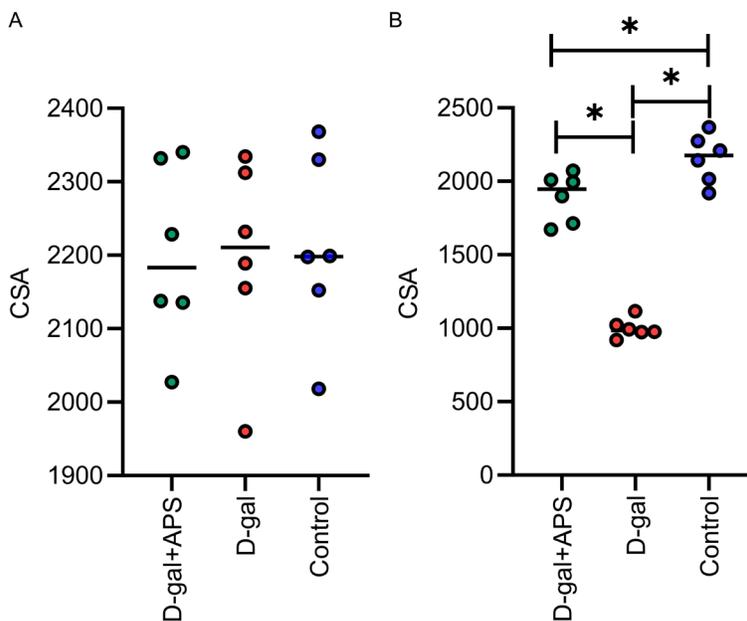
Figure 4. Effect of APS on gastrocnemius muscle CSA in D-gal-treated mice. A. There was no statistically significant difference in gastrocnemius muscle CSA among the three groups before intervention (n=6 for each group) (*P*>0.05). B. After intervention, the gastrocnemius muscle CSA decreased in the D-gal group compared to the control group, and APS treatment significantly increased gastrocnemius muscle CSA compared to the D-gal group (*P*<0.05). APS, Astragalus polysaccharide; CSA, cross-sectional area; D-gal, D-galactose.

protein extraction. After protein concentration was determined by the bicinchoninic acid (BCA) method, each group had approximately 20-30 μg of protein added for sodium dodecyl sulfate polyacrylamide gel electrophoresis (SDS-PAGE) (pre-run at 80 V followed by 120 V until separation). After electrophoresis, the proteins were transferred to a polyvinylidene fluoride (PVDF) membrane (100 V for 1 h), and blocked with 5% nonfat dry milk in Tris Buffered Saline with Tween-20 (TBST) for 1 h. Subsequently, the proteins were exposed to the LC3 and PINK1 primary antibodies, diluted to 1:1000, and incubated overnight at 4°C. The membranes were washed three times with TBST (each for 10 min) and incubated with the HRP-conjugated secondary antibody (diluted 1:5000) at room temperature for 1 h, followed by repeating the washing steps. Protein bands were visualized by enhanced chemiluminescence (ECL) detection using an exposure meter, and the LC3II/LC3I ratio and PINK1 relative expression were analyzed by ImageJ to calculate the relative level of protein expression.

Statistical methods

Statistical analyses were conducted utilizing SPSS version 26.0, while GraphPad Prism version 9.5.1 was used for plotting. The measurement data were assessed for normal distribution and presented as mean ± standard deviation. Intergroup differences were assessed through one-way analysis of variance (ANOVA), and post-hoc pairwise com-
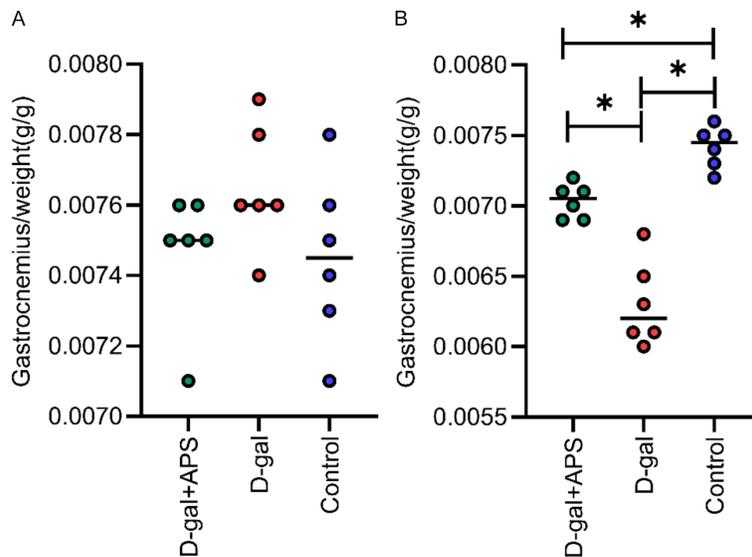
Figure 5. Effect of APS on Gastrocnemius Weight-to-Body Weight Ratio in D-gal-treated Mice. A. There was no statistically significant difference in gastrocnemius weight-to-body weight ratio among the three groups before intervention (n=6 for each group) (P>0.05). B. After intervention, the gastrocnemius weight-to-body weight ratio decreased in the D-gal group compared to the control group, and APS treatment significantly increased the gastrocnemius weight-to-body weight ratio compared to D-gal group (*P<0.05). APS, Astragalus polysaccharide; D-gal, D-galactose.

parisons were conducted utilizing least significant difference (LSD) test. A P-value of less than 0.05 was deemed statistically significant.

Results

Effects of APS on the grip strength of D-gal-treated mice

Following the establishment of the sarcopenia model, the mice were treated with APS for 8 weeks. Analysis of the grip strength test revealed that, compared to the control group, D-gal treatment resulted in a significant reduction in the grip strength of the mice (P<0.05). Conversely, treatment with APS significantly enhanced the grip strength of the mice subjected to D-gal treatment (P<0.05) (**Figure 1**).

Effects of APS on body mass, gastrocnemius weight, CSA, and gastrocnemius weight-to-body weight ratio in D-gal-treated mice

Before intervention, no significant differences were observed among the three groups in terms of body mass, gastrocnemius weight, gastrocnemius muscle CSA, and gastrocnemius weight-to-body weight ratio (all P>0.05). How-

ever, after intervention, D-gal treatment led to a significant reduction in body mass (**Figure 2**), gastrocnemius weight (**Figure 3**), gastrocnemius muscle CSA (**Figure 4**), and the gastrocnemius weight-to-body weight ratio (**Figure 5**) compared to the control group (all P<0.05). In contrast, APS treatment significantly improved these parameters in the D-gal-treated mice (all P<0.05).

Effects of APS on morphology of gastrocnemius muscle in D-gal-treated mice

Hematoxylin and eosin (H&E) staining was employed to assess the effect of APS treatment on the morphology of the gastrocnemius muscle in D-gal-treated mice. The results revealed that the muscle fibers in the control group were tightly arranged, with cells exhibiting a relatively full and rounded morphology (**Figure 6A** and **6B**). In contrast, the D-gal-treated mice showed significant morphological changes, including disorganized cell arrangement and widened myofiber gaps, indicative of muscle cell damage (**Figure 6C** and **6D**). However, APS treatment ameliorated these morphological changes, as demonstrated by more organized myofiber structures, reduced myofiber gaps, and alleviation of cell atrophy and senescence compared to the mice from D-gal groups (**Figure 6E** and **6F**).

Effects of APS on mitochondria in D-gal-treated mice

TEM analysis of the three groups (n=6) revealed that, compared to the control group (**Figure 7A**), mitochondria in the D-gal-treated group showed pronounced swelling, impaired morphology, a significant decrease in the number of autophagosomes, and disorganized myofibrils (**Figure 7B**). In contrast, APS treatment markedly reduced the number of swollen mitochondria, prevented cristae breakage and lysis, and increased the number of autophagosomes (**Figure 7C**).
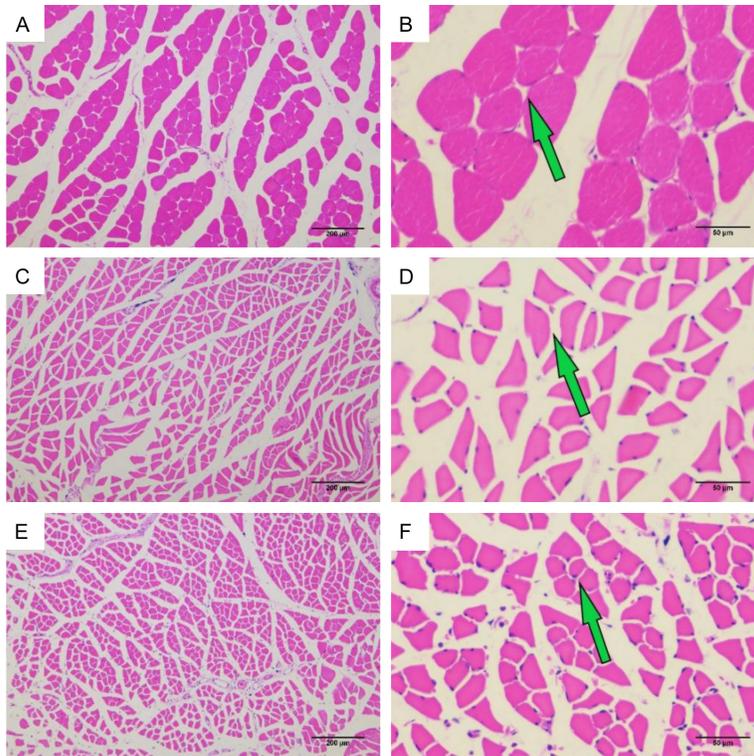
Figure 6. Effects of APS on the morphology of gastrocnemius muscle in mice induced by D-gal. (A, B) The muscle fibers in the control group were tightly arranged (A), with cells exhibiting a relatively full and rounded morphology (B); (C, D) The D-gal-treated mice showed significant morphological changes, including disorganized cell arrangement (C) and widened myofiber gaps (D); (E, F) APS treatment ameliorated these morphological changes, as demonstrated by transition of the muscle cell shape towards a more rounded form (E) and reduced myofiber gaps (F). APS, Astragalus polysaccharide; D-gal, D-galactose.

Effects of APS on the ultrastructure of the gastrocnemius muscle in D-gal-treated mice

TEM of the three groups (n=6) revealed a significant increase in the length of the sarcomere, I-bands, and H-bands in the gastrocnemius muscle tissues following D-gal treatment, as compared to the control group (**Figure 8A** and **8B**). In contrast, APS treatment markedly decreased the lengths of these bands (**Figure 8C**).

Effects of APS on protein expression of LC3II/LC3I and PINK1 in D-gal-treated mice

Western blot analysis revealed that D-gal treatment significantly reduced the protein expression levels of PINK1 and LC3II/LC3I in the gastrocnemius muscle tissues when compared to the control group. Conversely, APS treatment resulted in a significant increase in the expression levels of these proteins (**Figures 9-11**).

Discussion

D-galactose is a widely utilized agent in animal models to induce senescence [11, 12]. In this study, continuous administration of D-galactose significantly decreased the CSA of muscle tissue, lean body mass, gastrocnemius weight, and the ratio of gastrocnemius weight-to-body weight. Simultaneously, it markedly elevated the fat weight of the mice, indicating impaired muscle development in the model mice. Histological examination demonstrated that D-galactose tre-atment induced senescence and atrophy in the muscle cells, corroborating the damaging and aging effects of D-galactose on muscle tissues.

Electron microscopy further confirmed these findings, revealing the impaired morphology of muscle fibers in D-gal-treated mice, characterized by disordered arrangements and enlarged inter-fiber gaps. These observations suggest that the continuous D-gal administration effectively simulates sarcopenia, aligning with our experimental expectations and demonstrating the feasibility of this approach for investigating muscle degeneration and weakness.

The comprehensive results from morphological and ultrastructural analyses substantiate the validity of using D-gal as an inducer for sarcopenia in mice. Consequently, this model may serve as a valuable tool for exploring the pathophysiology of muscle aging and evaluating the potential therapeutic interventions.

In this study, the therapeutic potential of APS in D-gal-induced sarcopenia model mice was further investigated. The results demonstrated that APS treatment significantly increased the gastrocnemius weight, and the ratio of gastroc-
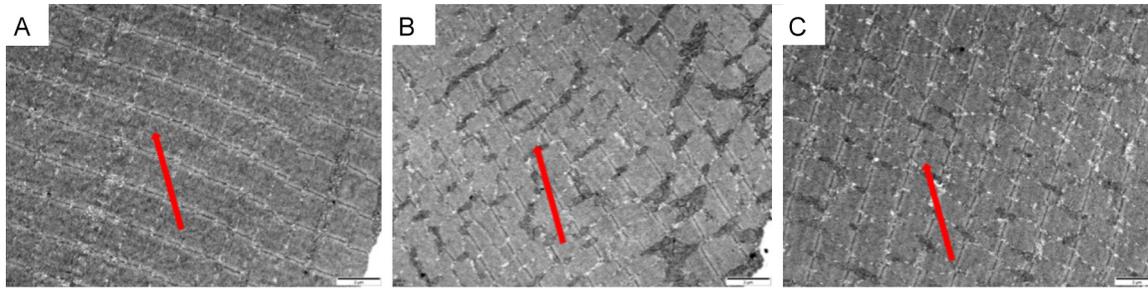
Figure 7. Effects of APS on mitochondria in D-gal-induced mice. Compared to the control group (A), mitochondria in the D-gal-treated group showed pronounced swelling, impaired morphology, and disorganized myofibrils (B); APS treatment markedly reduced the number of swollen mitochondria, prevented cristae breakage and lysis (C). APS, Astragalus polysaccharide; D-gal, D-galactose.
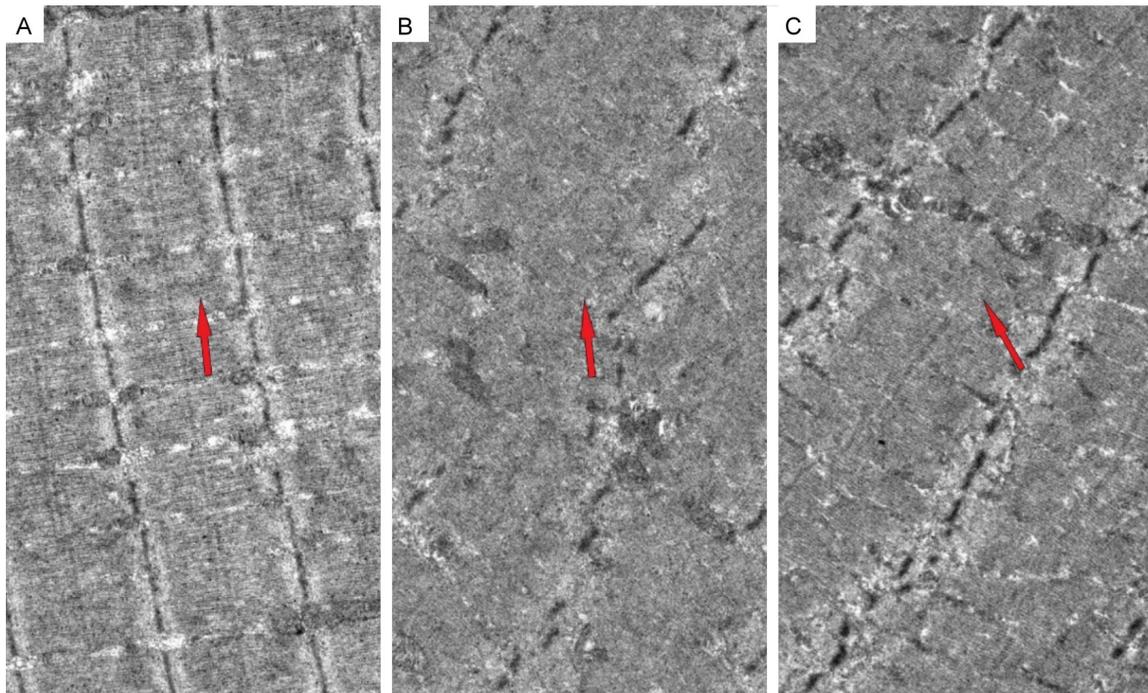
Figure 8. Effects of APS on the ultrastructure of gastrocnemius muscle in D-gal-induced mice. Compared to the control group (A), the D-gal-treated group exhibited a significant increase in the length of the sarcomere, I-bands, and H-bands in the gastrocnemius muscle tissues (B); APS treatment markedly decreased the lengths of these bands (C). APS, Astragalus polysaccharide; D-gal, D-galactose.
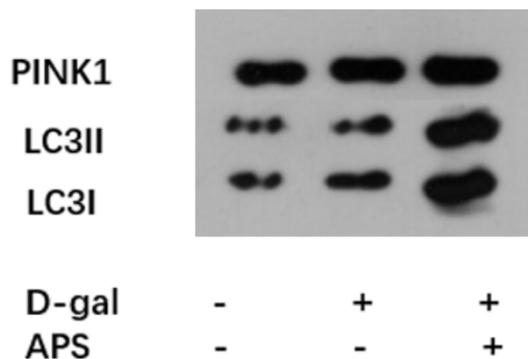
Figure 9. Effect of APS on protein expression of LC3II/LC3I and PINK1 in mice induced by D-gal. APS, Astragalus polysaccharide; D-gal, D-galactose.

nemius weight-to-body weight compared to the D-gal group. Morphological analyses revealed that APS significantly improved the growth and developmental morphology of myocytes, alleviated D-gal-induced myocyte senescence and atrophy, and increased the CSA of muscle fibers.

A review of the literature reveals a notable absence of prior studies specifically investigating the effects of APS on sarcopenia in both patients and animal models. However, a study by Kong et al. [13] explored the effects of APS in diabetic sarcopenia in rats, and their results showed that APS effectively improved the mor-
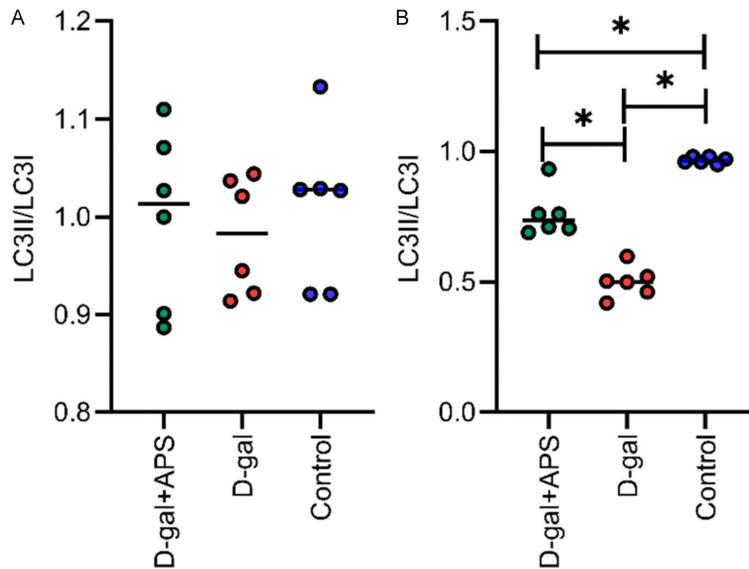
Figure 10. Effect of APS on LC3II/LC3I protein expression in D-gal-treated mice. A. There was no statistically significant difference in LC3II/LC3I protein expression among the three groups before intervention ($P>0.05$). B. After intervention, LC3II/LC3I protein expression decreased in the D-gal group compared to the control group, and APS treatment significantly increased LC3II/LC3I protein expression compared to D-gal group (*$P<0.05$). APS, Astragalus polysaccharide; D-gal, D-galactose.
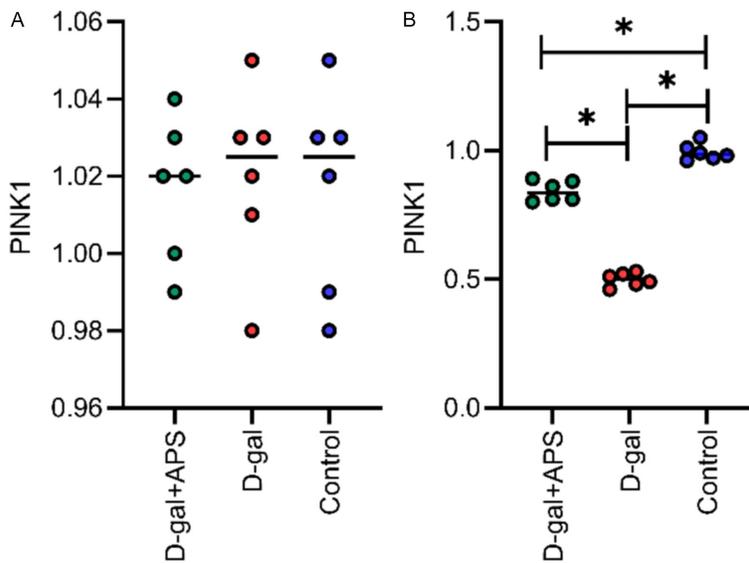
Figure 11. Effect of APS on PINK1 protein expression in D-gal-treated mice. A. There was no statistically significant difference in PINK1 protein expression among the three groups before intervention ($P>0.05$). B. After intervention, PINK1 protein expression decreased in the D-gal group compared to the control group, and APS treatment significantly increased PINK1 protein expression compared to D-gal group (*$P<0.05$). APS, Astragalus polysaccharide; D-gal, D-galactose.

and significantly decreased inflammatory exudation and the levels of inflammatory factors IL-6 and MMP-9, consistent with the results of this study.

The beneficial effects of APS observed in this study may be attributed to its complex composition, which includes various monosaccharides and dextrans. Dextrans are recognized as biological response modifiers that enhance immune function and reduce muscle atrophy. Furthermore, other studies [14, 15] have indicated that APS may upregulate the levels of antioxidant factors, thereby mitigating oxidative stress. This antioxidant property may represent one of the mechanisms by which APS exerts its protective effects against muscle degeneration.

To investigate the influence of APS on the progression of sarcopenia through mitochondrial autophagy, mitochondrial morphology was analyzed via electron microscopy, and protein expression levels were assessed. TEM revealed that APS mitigated mitochondrial damage in the myoblasts of D-gal-treated mice. Notably, APS treatment alleviated mitochondrial swelling, the loss of autophagosomes, and the disarray of myofibrils, suggesting that APS ameliorates D-gal-induced muscle tissue damage, aging, and atrophy by modulating mitochondrial autophagy.

Subsequent protein expression analysis revealed that D-gal treatment significantly reduced the levels of PINK1 and LC3II/LC3I proteins in the gastrocnemius muscle tissues,

phology of gastrocnemius muscle cells, increased cell volume, reduced intercellular gaps,

which were increased after APS treatment. The PINK1 signaling pathway is recognized for its role in regulating mitochondrial autophagy, and numerous studies have demonstrated that exercise interventions can both prevent and mitigate sarcopenia by modulating this pathway [16-18]. These findings imply that targeting mitochondrial autophagy may represent a promising strategy for the intervention of sarcopenia.

D-gal treatment effectively induced sarcopenia in mice, while the administration of APS improved the structure and function of muscle tissue in D-gal-treated mice. APS treatment increased the gastrocnemius weight and CSA of muscle fibers in the model mice, which may be attributed to its ability to promote mitochondrial autophagy. This study highlights the potential relationship between sarcopenia and mitochondrial autophagy, as evidenced by animal experiments, thereby providing new perspectives and approaches for the treatment of sarcopenia.

Nevertheless, this study has several limitations. Future research should endeavor to verify these findings through clinical trials to further elucidate the relationship between sarcopenia and mitochondrial autophagy. Such investigations will enhance our understanding and may ultimately lead to more effective therapeutic strategies for sarcopenia.

Acknowledgements

Disclosure of conflict of interest

None.

Address correspondence to: Qian Xiao, Department of Geriatrics, The First Affiliated Hospital of Chongqing Medical University, No. 1 Youyi Road, Yuanjiagang, Yuzhong District, Chongqing 400042, China. Tel: +86-023-68811360; E-mail: xiaoqian1956@126.com

References

[1] Damluji AA, Alfaraidhy M, AlHajri N, Rohant NN, Kumar M, Al Malouf C, Bahrainy S, Ji Kwak M, Batchelor WB, Forman DE, Rich MW, Kirkpatrick J, Krishnaswami A, Alexander KP, Gersten-blith G, Cawthon P, deFilippi CR and Goyal P. Sarcopenia and cardiovascular diseases. Circulation 2023; 147: 1534-1553.

[2] Sayer AA and Cruz-Jentoft A. Sarcopenia definition, diagnosis and treatment: consensus is growing. Age Ageing 2022; 51: afac220.

[3] Cho MR, Lee S and Song SK. A review of sarcopenia pathophysiology, diagnosis, treatment and future direction. J Korean Med Sci 2022; 37: e146.

[4] Smith C, Woessner MN, Sim M and Levinger I. Sarcopenia definition: does it really matter? Implications for resistance training. Ageing Res Rev 2022; 78: 101617.

[5] Coletta G and Phillips SM. An elusive consensus definition of sarcopenia impedes research and clinical treatment: a narrative review. Ageing Res Rev 2023; 86: 101883.

[6] Liang J, Zeng Z, Zhang Y and Chen N. Regulatory role of exercise-induced autophagy for sarcopenia. Exp Gerontol 2020; 130: 110789.

[7] Zeng Z, Liang J, Wu L, Zhang H, Lv J and Chen N. Exercise-induced autophagy suppresses sarcopenia through Akt/mTOR and Akt/FoxO3a signal pathways and ampk-mediated mitochondrial quality control. Front Physiol 2020; 11: 583478.

[8] Zhang J and Feng Q. Pharmacological effects and molecular protective mechanisms of astragalus polysaccharides on nonalcoholic fatty liver disease. Front Pharmacol 2022; 13: 854674.

[9] Jin J, Yang Z, Liu H, Guo M, Chen B, Zhu H, Wang Y, Lin J, Wang S and Chen S. Effects of acupuncture on the miR-146a-mediated IRAK1/TRAF6/NF-κB signaling pathway in rats with sarcopenia induced by D-galactose. Ann Transl Med 2023; 11: 47.

[10] Wijaya YT, Setiawan T, Sari IN, Park K, Lee CH, Cho KW, Lee YK, Lim JY, Yoon JK, Lee SH and Kwon HY. Ginsenoside Rd ameliorates muscle wasting by suppressing the signal transducer and activator of transcription 3 pathway. J Cachexia Sarcopenia Muscle 2022; 13: 3149-3162.

[11] Azman KF and Zakaria R. D-Galactose-induced accelerated aging model: an overview. Biogerontology 2019; 20: 763-782.

[12] Wang HH, Sun YN, Qu TQ, Sang XQ, Zhou LM, Li YX and Ren FZ. Nobiletin prevents d-galactose-induced C2C12 cell aging by improving mitochondrial function. Int J Mol Sci 2022; 23: 11963.

[13] Kong YH, Liu XB, Chang B and Juan W. Study on the mechanism of astragalus polysaccharide in reducing muscle atrophy in diabetic myopenia rats. Tianjin Journal of Traditional Chinese Medicine 2024; 41: 106-110.

[14] Zhang H, Qi G, Wang K, Yang J, Shen Y, Yang X, Chen X, Yao X, Gu X, Qi L, Zhou C and Sun H. Oxidative stress: roles in skeletal muscle atrophy. Biochem Pharmacol 2023; 214: 115664.

[15] Dzik KP and Kaczor JJ. Mechanisms of vitamin D on skeletal muscle function: oxidative stress, energy metabolism and anabolic state. Eur J Appl Physiol 2019; 119: 825-839.

[16] Lazarou M, Sliter DA, Kane LA, Sarraf SA, Wang C, Burman JL, Sideris DP, Fogel AI and Youle RJ. The ubiquitin kinase PINK1 recruits autophagy receptors to induce mitophagy. Nature 2015; 524: 309-314.

[17] Lin Q, Li S, Jiang N, Shao X, Zhang M, Jin H, Zhang Z, Shen J, Zhou Y, Zhou W, Gu L, Lu R and Ni Z. PINK1-parkin pathway of mitophagy protects against contrast-induced acute kidney injury via decreasing mitochondrial ROS and NLRP3 inflammasome activation. Redox Biol 2019; 26: 101254.

[18] Liu Z, Wang M, Wang X, Bu Q, Wang Q, Su W, Li L, Zhou H and Lu L. XBP1 deficiency promotes hepatocyte pyroptosis by impairing mitophagy to activate mtDNA-cGAS-STING signaling in macrophages during acute liver injury. Redox Biol 2022; 52: 102305.